

# Security-Constrained Unit Commitment in Presence of Lithium-Ion Battery Storage Units Using Information-Gap Decision Theory

Abdollah Ahmadi<sup>ID</sup>, *Student Member, IEEE*, Ali Esmaeel Nezhad, *Student Member, IEEE*, and Branislav Hredzak<sup>ID</sup>, *Senior Member, IEEE*

**Abstract**—This paper proposes a robust framework for the security-constrained unit commitment (SCUC) of generating units, in the presence of lithium-ion battery energy storage units, using the information-gap decision theory (IGDT) technique. In the suggested model, the degradation cost of the battery storage units has been considered in the objective function as a highly influencing factor in the operation of such storage units. The framework is independent of probability density functions or membership of sets and enables the system operator to adjust the conservatism of the operating strategy (between overconservative and reckless) against the load demand uncertainty. In this respect, the SCUC model has been presented within a day-ahead scheduling problem on the hourly basis using mixed-integer linear programming. Finally, the proposed framework has been simulated on a typical 6-bus test system as well as IEEE 24-bus and IEEE 118-bus systems to verify the efficiency and the effectiveness of the model using the IGDT technique.

**Index Terms**—Energy storage systems (ESSs), information-gap decision theory (IGDT), load uncertainty, security-constrained unit commitment (SCUC).

## I. INTRODUCTION

THERE is an increasing trend in the installation of energy storage systems (ESSs) during last decades. According to Electric Power Research Institute, about 10% to 20% of the installed capacity in the generation sector will consist of ESSs by 2025 [1]. In electric power systems, ESSs provide various services such as tracking variation in power generation, meeting changes in the load demand, and mitigating the impacts of renewable energies' uncertainty on power systems [2], [3]. They can also be used for frequency control by injecting/absorbing power to/from the power network during peak/off-peak hours and participating in the frequency regulation service markets

[4]. Based on the National Renewable Energy Laboratory projections, tracking the load demand fluctuations while provided other ancillary services will be very challenging [5].

This paper proposes a robust framework for security-constrained unit commitment (SCUC) of generating units in the presence of energy storage units, considering the load uncertainty and the battery degradation cost.

The main causes of uncertainties in electric power systems are volatile renewable energy sources (RESs), load demand, and energy prices. Effective tools must be applied to handle the uncertainties. So far, mostly, stochastic optimization has been used to model the uncertain parameters [6]. However, there are two main drawbacks associated with the stochastic optimization, first, exact probability distribution of the data is required; and second, the accuracy is highly dependent upon the number of scenarios, which can excessively enlarge the size of the problem. The information-gap decision theory (IGDT) technique is an alternative method that avoids these drawbacks and can provide a solution that is robust against uncertainties, such as the forecasting errors. The IGDT was first proposed by Ben-Haim [7]. The IGDT technique has been widely used in problems related to electric power systems. Electric energy procurement problem for large-scale consumers was solved in [8] by proposing a risk-based model using the IGDT technique. In [9], the IGDT was utilized to tackle the uncertainty in selecting energy resources of distribution network operators. The problem of dynamic transmission expansion planning, within a multiobjective optimization framework, was solved using the IGDT technique in [10]. Kazemi *et al.* [11] presented a risk-based framework employing the IGDT technique for the bidding strategy of an electric utility managing a retailer and generating units to maximize the profit. The optimal power flow (OPF) problem for ac/dc power systems in the presence of high-voltage direct current connected wind farms was formulated and solved using the IGDT method in [12]. Charwand *et al.* [13] used the IGDT for the short-term hydrothermal scheduling period in the presence of the load demand uncertainty. An enhanced mixed-integer quadratic constraint programming framework for distribution systems' restoration proposed in [14] used the IGDT technique to characterize the load demand uncertainty as well as the distributed generations' output. The application of the IGDT technique to characterize the uncertainty of renewable power generation within the context of ac OPF was investigated in [15].

Manuscript received July 27, 2017; revised December 3, 2017 and January 24, 2018; accepted February 14, 2018. Date of publication March 6, 2018; date of current version January 3, 2019. Paper no. TII-17-1655. (Corresponding author: Abdollah Ahmadi.)

A. Ahmadi and B. Hredzak are with the Australian Energy Research Institute and the School of Electrical Engineering and Telecommunications, University of New South Wales, Sydney, NSW 2032, Australia (e-mail: a.ahmadi@student.unsw.edu.au; b.hredzak@unsw.edu.au).

A. Esmaeel Nezhad is with the Department of Electrical, Electronic, and Information Engineering, University of Bologna, Bologna 40126, Italy (e-mail: ali.esmaeelnezhad.1989@ieeee.org).

Digital Object Identifier 10.1109/TII.2018.2812765

In [16], the IGDT method was utilized to determine the day-ahead risk-constrained bidding/offering strategy for a merchant compressed air energy storage plant.

Energy management of ESSs in power systems has also attracted a lot of attention. In [17], an optimization framework for energy management of a hybrid power system comprising wind power generation and battery ESSs was presented. A two-scale dynamic programming method was used to plan batteries' setpoint trajectory over a long period considering wind speed predictions over a short-term period. However, the impact of battery degradation cost on the performance of the model was not considered. In [18], a framework for short-term scheduling of power systems including thermal generators and batteries was developed. The presented model emphasized the relationship between the battery cycling and long-term costs of batteries. The framework took into account the short-term cost model including the battery cycling and the depth of discharge (DoD). However, the load forecast uncertainty was not taken into account in the proposed model. A flexible energy management system, considering optimized charge/discharge periods of batteries during one day was proposed in [19]. A two-stage programming method, with the objective function as the profit maximization, was used. However, the load forecast inaccuracy was neglected. A coordinated operation strategy for a wind farm together with a battery ESS to mitigate the undispachability of the wind power generation was presented in [20]. Stochastic programming was employed to characterize the uncertainty of the problem. A two-step optimization framework for integration of intermittent RESs with ESSs in the context of stochastic unit commitment (UC) and economic dispatch was proposed in [21]. **Table I** represents a comparison between the proposed framework and the existing methods for the UC problem. It is noteworthy that the following four criteria have been taken into account for this comparison: first, the uncertain input data; second, the method used for characterizing the uncertainty; third, the type of problem whether it is UC or SCUC; and fourth, the application of ESSs.

In this respect, Parvania *et al.* [22] presented a deterministic framework for the SCUC in the presence of EESSs without considering the degradation costs using the mixed-integer programming technique. Blanco and Morales [23] have solved the stochastic SCUC problem using the scenario-based optimization and clustering the scenarios that characterize the related probability density functions. Using this technique, the conservatism degree can be adjusted by determining the number of partitions into which the sample space of the uncertain parameter is split. Zhang *et al.* [24] employed the chance-constrained two-stage stochastic programming technique to solve the SCUC problem taking into account the uncertainties due to the load demand and wind power. Shao *et al.* [25] utilized a robust optimization method with flexible uncertainty set to characterize the uncertainty of the wind power generation in the context of the SCUC problem. The nonparametric neural network-based prediction intervals are used in [26] to forecast the uncertainty quantification of RESs and Monte Carlo simulation has been used to generate the scenarios of the wind speed in the context of the stochastic SCUC. Wang *et al.* [27] proposed a

new model based on the chance-constrained programming and goal programming to accommodate the wind power intermittency in the SCUC problem. Lorca and Sun [28] presented a multistage adaptive robust optimization for the SCUC problem taking into consideration the temporal and spatial correlations of wind and solar power in the Polish 2736-bus system. Aghaei *et al.* [29] used the IGDT technique for the UC of combined heat and power generation plants considering the market price uncertainty.

However, it should be noted that no exceptional and magic method is available for characterizing the uncertainty of the load demand within the SCUC model.

None of the above-mentioned works applied the IGDT method to the SCUC of generating units in the presence of large-scale battery energy storage without any assumption on the load uncertainty and considering the battery degradation cost. Hence, the main contributions of the paper are as follows.

- 1) A robust framework for the SCUC in the presence of battery ESSs, based on the IGDT technique. The framework is independent of probability density functions or membership of sets.
- 2) A model optimizing the robustness of a decision-making strategy.
- 3) Optimization of the decision-making strategy robustness (instead of cost) without any assumption on the load uncertainty and considering the battery degradation cost.
- 4) A mathematical model for finding a balance between overconservative and reckless strategy.

The remainder of the paper is organized as follows: The mathematical modeling of the problem with IGDT technique is described in Section II. Section III presents and analyzes simulation results, and Section IV concludes the paper.

## II. MATHEMATICAL MODEL

### A. IGDT Technique

This section provides a brief introduction to the IGDT technique. Each IGDT-based decision-making problem requires system model, performance necessities, and uncertainty modeling as follows.

- 1) *System model*: In this paper, the system model  $R(x, \psi)$  represents the total operating cost function in the presence of large ESSs, indicated by a set of decision variables  $x$ , and the uncertain parameter  $\psi$ .  $R(x, \psi)$  evaluates the system's response taking into consideration the decision made.
- 2) *Performance necessities*: The performance necessities (expectancy) of the problem can be stated as a cost or any other function, and assessed by the robustness function RF

$$\text{RF}(x, R_c) = \max_{\alpha} \left\{ \alpha : \begin{array}{l} \text{maximum operating cost not} \\ \text{higher than a predetermined cost} \end{array} \right\} \quad (1)$$

where  $\alpha$  denotes the uncertainty horizon of uncertain parameter  $\psi$ . The robustness function finds the maximum

**TABLE I**  
COMPARISON BETWEEN THE EXISTING METHODS AND THE PROPOSED METHOD

Reference	Uncertain phenomenon			Uncertainty modeling					Type of Problem		Storage unit
	Load	Price	RES	Deterministic	Stochastic	Robust	Chance-constrained	IGDT	SCUC	UC	
[22]				*					*		*
[2]			*		*					*	*
[23]			*		*				*		
[24]	*		*				*		*		
[25]			*			*			*		
[26]			*		*				*		
[27]			*				*		*		
[28]			*			*			*		*
[29]		*						*		*	
Proposed framework	*							*	*		*

value of  $R(x, \psi)$  with the operating cost not higher than a predetermined cost  $R_c$ . The robustness function indicates the system's tolerance to the uncertainty and also its immunity against high operating costs. The mathematical representation of the robustness function of the IGDT technique is

$$\begin{aligned} \text{RF}(x, R_c) &= \max_{\alpha} \{ \alpha : \max R(x, \psi) \\ &\leq R_c = (1 + \sigma)R_0 \} \end{aligned} \quad (2)$$

where  $\sigma$  is the cost deviation factor and  $R_0$  is the base cost. The decision is robust to uncertainties for a large value of  $\text{RF}(x, R_c)$ , whereas the small value of  $\text{RF}(x, R_c)$  implies that the decision will be crisp, with high deviation in the uncertain parameter  $\psi$ .

- 3) *Uncertainty model*: In this paper, the parameter uncertainty is modeled using the envelope-bound model [30]. The IGDT technique attempts to characterize the gap between the specified and unspecified values as a function of some specified parameters such as the expected value of the uncertain parameter. The envelope-bound model based modeling of the uncertain parameter can be stated as

$$\begin{aligned} \psi &\in H(\alpha, \hat{\psi}) \\ H(\alpha, \hat{\psi}) &= \left\{ \psi : \left| \frac{\psi - \hat{\psi}}{\hat{\psi}} \right| \leq \alpha \right\} \end{aligned} \quad (3)$$

where  $\hat{\psi}$  is the expected value of  $\psi$ .  $H(\alpha, \hat{\psi})$  is the set of values belonging to the variations of  $\psi$  with respect to  $\hat{\psi}$ , less than  $\alpha\hat{\psi}$ . In this paper, the uncertain parameter  $\psi$  is the hourly load demand. In case the decision maker intends to be risk averse, the uncertainty horizon should be maximized to obtain the required performance.

### B. Problem Formulation

This section describes the mathematical model of the proposed problem within the context of mixed-integer linear programming. First, the deterministic model  $z$  is proposed. The objective function of the SCUC problem (system model) to be

minimized is

$$\begin{aligned} R(x, \psi) &= \min \left[ \sum_{t \in NT} \left[ \sum_{i \in NG} \left( C_i^{\min} I_{it} \right. \right. \right. \\ &\quad \left. \left. \left. + \sum_{n=1}^{NN_i} \mu_{it}^n P_{it}^n + \text{SU}_{it} + \text{SD}_{it} \right) \right] \right] \\ i &= 1, 2, \dots, NG; \quad t = 1, 2, \dots, NT; \quad n = 1, 2, \dots, NN_i \end{aligned} \quad (4)$$

$$\begin{aligned} P_{it} &= P_{it}^{\min} I_{it} + \sum_{n=1}^{NN_i} P_{it}^n \\ i &= 1, 2, \dots, NG; \quad t = 1, 2, \dots, NT; \quad n = 1, 2, \dots, NN_i \end{aligned} \quad (5)$$

$$\begin{aligned} 0 &\leq P_{it}^n \leq P_i^{n, \max} \\ i &= 1, 2, \dots, NG; \quad t = 1, 2, \dots, NT; \quad n = 1, 2, \dots, NN_i \end{aligned} \quad (6)$$

$$\begin{aligned} P_i^{\min} I_{it} &\leq P_{it} \leq P_i^{\max} I_{it} \\ i &= 1, 2, \dots, NG; \quad t = 1, 2, \dots, NT \end{aligned} \quad (7)$$

$$\begin{aligned} \text{SU}_{it} &\geq K_i (I_{it} - I_{i(t-1)}) \\ i &= 1, 2, \dots, NG; \quad t = 1, 2, \dots, NT \end{aligned} \quad (8)$$

$$\begin{aligned} \text{SD}_{it} &\geq J_i (I_{i(t-1)} - I_{it}) \\ i &= 1, 2, \dots, NG; \quad t = 1, 2, \dots, NT; \quad n = 1, 2, \dots, NN_i \end{aligned} \quad (9)$$

$$\begin{aligned} \sum_{t'=t}^{t+T_i^{\text{on}}-1} I_{it'} &\geq T_i^{\text{on}} (I_{it} - I_{i(t-1)}) \\ i &= 1, 2, \dots, NG; \quad t = 1 \dots NT - T_i^{\text{on}} + 1 \end{aligned} \quad (10)$$

$$\begin{aligned} \sum_{t'=t}^{t+T_i^{\text{off}}-1} (1 - I_{it'}) &\geq T_i^{\text{off}} (I_{i(t-1)} - I_{it}) \\ i &= 1, 2, \dots, NG; \quad t = 1 \dots NT - T_i^{\text{off}} + 1 \end{aligned} \quad (11)$$

$$\begin{aligned} P_{it} - P_{i(t-1)} &\leq \text{RU}_i I_{i(t-1)} + \text{SUR}_i (I_{it} - I_{i(t-1)}) \\ i &= 1, 2, \dots, NG; \quad t = 1, 2, \dots, NT \end{aligned} \quad (12)$$

$$P_{i(t-1)} - P_{it} \leq \text{RD}_i I_{it} + \text{SDR}_i (I_{i(t-1)} - I_{it})$$

$$i = 1, 2, \dots, NG; \quad t = 1, 2, \dots, NT \quad (13)$$

$$E_{e(t+1)}^{\text{CT}} = E_{et}^{\text{CT}} + \left[ \eta_e^{D,\text{CT}} C_{et}^{\text{CT}} - \frac{1}{\eta_e^{C,\text{CT}}} D_{et}^{\text{CT}} \right]$$

$$e = 1, 2, \dots, NE; \quad t = 1, 2, \dots, NT \quad (14)$$

$$E_{e,0}^{\text{CT}} = E_{e}^{\text{CT},\text{initial}} \quad e = 1, 2, \dots, NE \quad (15)$$

$$E_{e}^{\text{CT},\text{min}} \leq E_{et}^{\text{CT}} \leq E_{e}^{\text{CT},\text{max}},$$

$$e = 1, 2, \dots, NE; \quad t = 1, 2, \dots, NT \quad (16)$$

$$D_{et}^{\text{CT}} \leq U_{et}^{D,\text{CT}} \text{PR}_e^{\text{CT}}$$

$$e = 1, 2, \dots, NE; \quad t = 1, 2, \dots, NT \quad (17)$$

$$C_{et}^{\text{CT}} \leq U_{et}^{C,\text{CT}} \text{PR}_e^{\text{CT}}$$

$$e = 1, 2, \dots, NE; \quad t = 1, 2, \dots, NT \quad (18)$$

$$U_{et}^{D,\text{CT}} + U_{et}^{C,\text{CT}} \leq 1$$

$$e = 1, 2, \dots, NE; \quad t = 1, 2, \dots, NT \quad (19)$$

$$-\text{RD}_{et}^{\text{CT}} \leq D_{et}^{\text{CT}} - D_{e(t-1)}^{\text{CT}} \leq \text{RD}_{et}^{\text{CT}}$$

$$e = 1, 2, \dots, NE; \quad t = 1, 2, \dots, NT \quad (20)$$

$$-\text{RC}_{et}^{\text{CT}} \leq C_{et}^{\text{CT}} - C_{e(t-1)}^{\text{CT}} \leq \text{RC}_{et}^{\text{CT}}$$

$$e = 1, 2, \dots, NE; \quad t = 1, 2, \dots, NT \quad (21)$$

$$\sum_{i \in NG_b} P_{it} + \sum_{e \in NE_b} (D_{et}^{\text{CT}} - C_{et}^{\text{CT}}) - P_{bt}^D = \sum_{l \in NL_b} \text{PL}_{lt}$$

$$b = 1, 2, \dots, NB; \quad t = 1, 2, \dots, NT \quad (22)$$

$$\text{PL}_{lt} = B_l (\theta_{lt}^S - \theta_{lt}^R)$$

$$l = 1, 2, \dots, NL; \quad t = 1, 2, \dots, NT \quad (23)$$

$$-\text{PL}_{lt}^{\text{max}} \leq \text{PL}_{lt} \leq \text{PL}_{lt}^{\text{max}}$$

$$l = 1, 2, \dots, NL; \quad t = 1, 2, \dots, NT \quad (24)$$

$$\sum_{i \in NG} P_{it}^{\text{max}} I_{it} \geq \text{SRR}_t + \sum_{b \in NB} P_{bt}^D$$

$$i = 1, 2, \dots, NG; \quad t = 1, 2, \dots, NT; \quad b = 1, 2, \dots, NB. \quad (25)$$

In (4),  $C_i^{\text{min}}(\$)$  is the minimum production cost of the thermal unit  $i$ ,  $I_{it}$  is a binary variable indicating the commitment status of unit  $i$ ,  $\mu_{it}^n$  is the slope of segment  $n$  pertaining to the cost function of unit  $i$  at time  $t$ ,  $P_{it}^n(\text{MW})$  is the power output of thermal unit  $i$  in segment  $n$  at time  $t$ .  $NT$  and  $NG$  are the total hours of the scheduling period and the total number of thermal generating units, respectively.  $NN_i$  indicates the total number of segments of the piecewise linearized cost function of the thermal unit  $i$ . The start-up (SU) and shut-down (SD) costs of the thermal unit  $i$  at time  $t$  all in (\$) are denoted by  $\text{SU}_{it}$  and  $\text{SD}_{it}$ , respectively. The linearized formulation for power generation of the thermal unit  $i$  at time  $t$  is given by (5).

The presented SCUC problem is subject to several equality and inequality constraints. The constraints for the thermal power generation in each segment  $n$  and the power generation limits at each hour of the scheduling period are as (6) and (7).

$P_{it}(\text{MW})$  is the power generation of the thermal unit  $i$  at time  $t$ , while  $P_i^{\text{min}}$  and  $P_i^{\text{max}}$  indicate the lower and upper bounds of the power generation of unit  $i$  in MW, respectively.

The linear  $\text{SU}_{it}$  and  $\text{SD}_{it}$  costs are given as (8) and (9), respectively, where  $K_i$  and  $J_i$  denote the SU and SD costs (\$) of the thermal unit  $i$ . Inequality (10) depicts the minimum up-time (MUT) limit of the problem (hour) and (11) is the linear formulation of minimum down-time (MDT) limit (hour) of the thermal generating units, where  $T_i^{\text{on}}$  and  $T_i^{\text{off}}$  are the MUT (hour) and the MDT (hour) of the thermal unit  $i$ . The ramp-up limit (RU) and the ramp-down limit (RD) of the thermal generating units are given by (12) and (13), respectively.  $\text{RU}_i$ ,  $\text{RD}_i$ ,  $\text{SUR}_i$ , and  $\text{SDR}_i$  are the Ramp-Up, ramp-down, start-up ramp, and shut-down ramp limits of the thermal unit  $i$  all in (MW/h), respectively. The energy balance equation of the ESSs is given by (14), taking into account the charging/discharging efficiency of the ESS.  $E_{et}^{\text{CT}}$  (MWh) is the energy stored in the battery  $e$  at time  $t$ .  $C_{et}^{\text{CT}}$  and  $D_{et}^{\text{CT}}$  are the charging and discharging powers (MW).  $\eta_e^{C,\text{CT}}$  and  $\eta_e^{D,\text{CT}}$  are the charging and discharging efficiencies of the ESS  $e$ . The constraint on the initial energy stored in the ESS is given by (15). Inequality (16) limits the minimum and maximum energy stored in the ESS.  $E_{e}^{\text{CT},\text{initial}}$  (MWh) is the initial energy stored in the ESS  $e$ .  $E_{e}^{\text{CT},\text{min}}$  (MWh) and  $E_{e}^{\text{CT},\text{max}}$  (MWh) are the minimum and maximum energy that can be stored in the ESS  $e$ , respectively. The maximum charging and discharging rates of the ESS are modeled as (17) and (18), respectively.  $\text{PR}_e^{\text{CT}}$  (MW) is the power rating of the ESS  $e$ .  $U_{et}^{D,\text{CT}}$  and  $U_{et}^{C,\text{CT}}$  are binary variables specifying discharging and charging states of the ESS  $e$ , respectively. When both binary variables are zero, the operating mode is idle. The discharging and charging ramp rates of the ESS are limited by (20) and (21), respectively.  $\text{RC}_{et}^{\text{CT}}$  (MW/h) and  $\text{RD}_{et}^{\text{CT}}$  (MW/h) indicate the charging and discharging ramp rates of the ESS  $e$ , respectively. It is assumed that the electrical load demand must be fully supplied and no-load curtailment is allowed. Hence, the power balance equation is stated as (22).  $P_{bt}^D$  (MW) and  $\text{PL}_{lt}$  (MW) are the load demand at bus  $b$  and power flow of line  $l$  at time  $t$ , respectively.

The power flow through transmission lines is given by (23), whereas (24) assigns the maximum capacity of transmission lines. The amount of the spinning reserve required at each scheduling period is determined by (25).  $B_l$  is the susceptance of line  $l$ .  $\theta_{lt}$  is the voltage angle with superscripts  $S$  and  $R$  denoting sending and receiving buses, respectively.  $\text{PL}_{lt}^{\text{max}}$  is the maximum capacity of transmission line  $l$  and  $\text{SRR}_t$  is the spinning reserve requirement at time  $t$ .

### C. Battery Degradation Cost

One of the most significant factors that has to be taken into consideration, when employing batteries in the SCUC problem, is the battery degradation cost. Aging mechanism of the lithium-ion batteries is a complex process [31], [32]. So far, several



research works have developed several models for degradation costs of lithium-ion batteries. In this respect, Farzin *et al.* [33] have modeled the battery degradation cost as a series of equal payments during battery cycle life and a scheme is presented to calculate the associated wear price based on engineering economics principles. Zhou *et al.* [34] have utilized ambient temperature and DoD to calculate the degradation cost of the battery. Furthermore, DoD and lifetime and the long-term costs of batteries have been used in [35] to model the degradation cost.

One of the most important battery performance criteria is the battery's cycle life, which is defined as the number of charging/discharging cycles the battery can perform before its capacity falls below 80% of its initial capacity [36], [37]. The relationship between the cycle life and DoD is logarithmic. The number of cycles yielded by a battery goes up exponentially for the shallower DoD [36], [37]. Fig. 1 illustrates the cycle life versus DoD for a lithium-ion battery [38].

According to [36] and [37], the battery degradation cost can be stated as

$$C_{e,D} = \frac{\text{Battery replacement cost}}{\text{Total energy throughput during lifecycle}}. \quad (26)$$

The above relationship can be mathematically represented as [39]

$$C_{e,D} = \frac{C_e E_e^{\max}}{2L_e(\text{DoD}_e)E_e^{\max}\text{DoD}_e}, \quad e = 1, 2, \dots, NE. \quad (27)$$

In (27),  $C_{e,D}$  ( $\$/\text{kWh}$ ) is the cost of the battery and  $E_e^{\max}$  is the battery's capacity.  $L_e$  is the battery lifetime in terms of cycle life as a function of  $\text{DoD}_e$ . The factor of 2, in the denominator of (27), accounts for the degradation cost both due to charging and discharging. Thus, the objective function of the SCUC problem (4) can be rewritten, by taking into account the battery degradation cost, as

$$R(x, \psi) = \min \left[ \sum_{t \in NT} \left[ \sum_{i \in NG} \left( C_i^{\min} I_{it} + \sum_{n=1}^{NN_i} \mu_{it}^n P_{it}^n \right) + \sum_{e \in NE} C_{e,D} (D_{et}^{\text{CT}} + C_{et}^{\text{CT}}) \right] \right] \quad (28)$$

$i = 1, 2, \dots, NG; \quad t = 1, 2, \dots, NT; \quad n = 1, 2, \dots, NN_i;$   
 $e = 1, 2, \dots, NE$

and (5)–(27).

#### D. IGDT-Based Modeling

The objective of the IGDT is to maximize the uncertainty horizon  $\alpha$ , which can be stated as

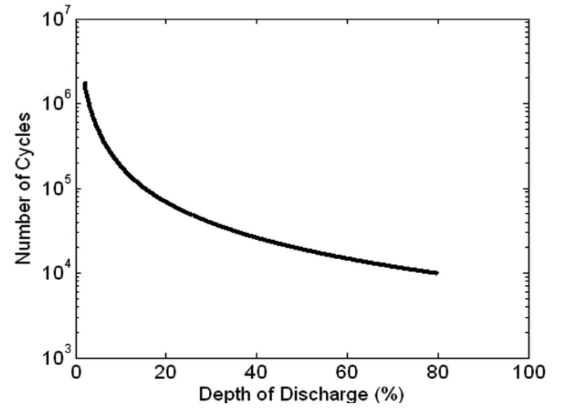


Fig. 1. DoD versus cycle life of a lithium-ion battery [38].

$$\text{RF}(x, R_c) = \max \alpha \quad (29)$$

s.t.

$$\max R(x, \psi) =$$

$$\max \left[ \sum_{t \in NT} \left[ \sum_{i \in NG} \left( C_i^{\min} I_{it} + \sum_{n=1}^{NN_i} \mu_{it}^n P_{it}^n \right) + \sum_{e \in NE} C_{e,D} (D_{et}^{\text{CT}} + C_{et}^{\text{CT}}) \right] \right] \leq (1 + \sigma) R_0 \quad (30)$$

$$b = 1, 2, \dots, NB, \quad t = 1, 2, \dots, NT,$$

$$e = 1, 2, \dots, NE, \quad l = 1, 2, \dots, NL$$

$$P_{bt}^D \leq (1 + \alpha) \tilde{P}_b^D, \quad b = 1, 2, \dots, NB, \quad t = 1, 2, \dots, NT \quad (31)$$

$$P_{bt}^D \geq (1 - \alpha) \tilde{P}_b^D, \quad b = 1, 2, \dots, NB, \quad t = 1, 2, \dots, NT \quad (32)$$

and (5)–(27).

Equation (30) represents the cost function's robustness to the largest deviations in the load demand  $\psi$ . Assuming the uncertainty horizon  $\alpha$  in the load demand, the robust mathematical formulation considering the highest load level can be stated as follows:

Equations (29) and (30)

s.t.

$$\sum_{i \in NG_b} P_{it} + \sum_{e \in NE_b} (D_{et}^{\text{CT}} - C_{et}^{\text{CT}}) - (1 + \alpha) P_{bt}^D = \sum_{l \in NL_b} PL_{lt}$$

$$b = 1, 2, \dots, NB, \quad t = 1, 2, \dots, NT,$$

$$e = 1, 2, \dots, NE, \quad l = 1, 2, \dots, NL \quad (33)$$

and (5)–(21), (23)–(27).

### III. SIMULATION RESULTS

This section presents simulation results obtained from implementing the proposed framework on a 6-bus test system as well as a modified IEEE 24-bus and 118-bus test systems. The

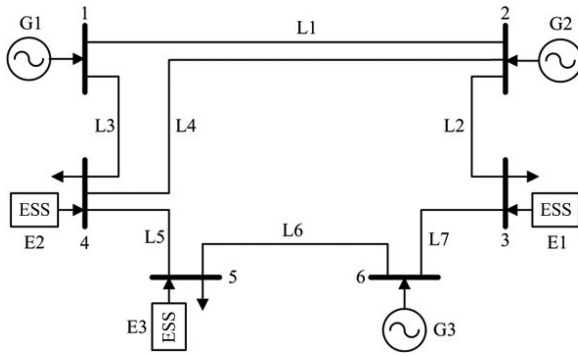


Fig. 2. 6-bus test system with battery [22].

TABLE II  
COMMITMENT STATUS OF THE THERMAL UNITS (BASE CASE)

Unit	Hours (1–24)
G1	111111111111111111111111
G2	000000000111111100000000
G3	000000111111111111111111

scheduling horizon is 24 h on the hourly basis. The ESS is a lithium-ion battery from Dynapower [40]. The battery degradation cost has been calculated as \$50/MWh, and the initial energy stored in the ESS has been selected as 50% of the battery capacity. The presented problems have been solved using CPLEX solver in GAMS software running on a laptop computer with Core i5 CPU and 4GB RAM.

### A. 6-Bus Test System

The transmission lines and generating units' data from [22] were used in the simulation. Fig. 2 shows the single-line diagram of the system with ESSs. The proposed problem is first solved using a deterministic framework, without any load forecast uncertainty, and is named "base case." In the base case, the objective is set to minimize the total operating cost with three ESSs installed at the load buses, as reported in [22]. The total ESS capacity is 10% of the peak load, i.e., 28 MWh. The obtained cost of the base case is \$93 325. Table II illustrates the commitment status of the thermal generating units. The thermal generating unit 1 (G1) is committed over all scheduling periods due to its lower cost as compared to others. The thermal generating unit 3 (G3) is committed over 18 h of the scheduling horizon, due to its lower cost than the thermal unit 2 (G2). The thermal power generation of the system is shown in Fig. 3.

Next, the load forecast uncertainty is taken into account. This case is named "robust case." The cost deviation factor  $\sigma$  is changed from 0.1 to 0.5 in steps of 0.1, to evaluate different operating strategies. The higher the value of  $\sigma$ , the higher operating cost that can be tolerated. Fig. 4 illustrates a variation of the load robustness  $\alpha$  versus the cost deviation factor  $\sigma$ .

Accordingly, the variation of the robustness cost versus the load robustness is shown in Fig. 5. As the cost increases, larger deviation in the load forecast uncertainty can be tolerated. In

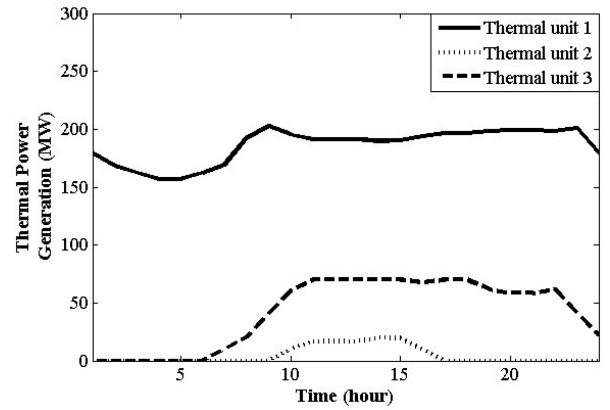


Fig. 3. Thermal power generation schedule in the base case ( $\alpha = 0$ , 6-bus system).

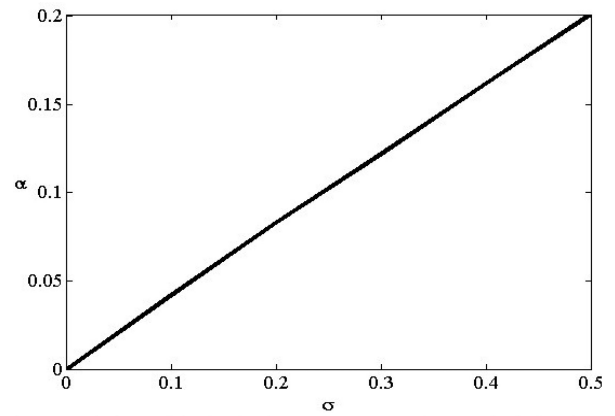


Fig. 4. Variations of the load robustness  $\alpha$  versus the cost deviation factor  $\sigma$  (6-bus system).

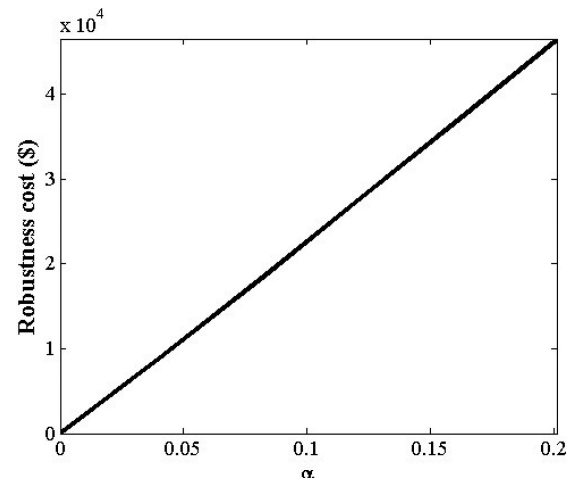
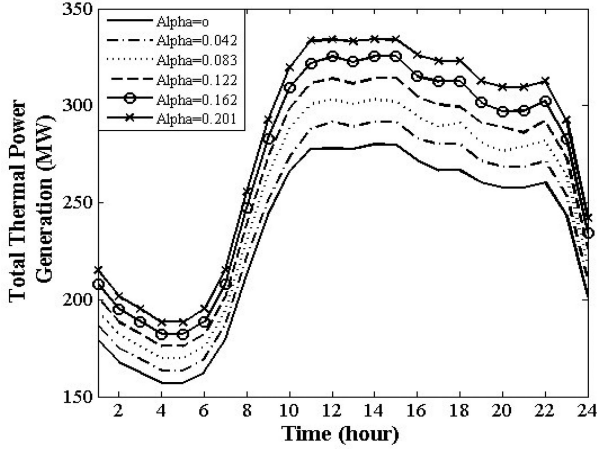


Fig. 5. Variation of the robustness cost versus the load robustness  $\alpha$  (6-bus system).

this respect, this paper models a risk-averse system operator by assuming the worst case scenario, i.e., the cost deviation factor of  $\sigma = 0.5$ . This means that operating cost of up to 1.5 times greater than the base cost can be tolerated by the system operator in order to accommodate the maximum uncertainty. This corresponds to the total operating cost of \$140 220 and the load

**TABLE III**  
COMMITMENT STATUS OF THERMAL UNITS ( $\sigma = 0.3, \alpha = 0.122$ )

Unit	Hours (1–24)
G1	111111111111111111111111
G2	000000001111111111111110
G3	000001111111111111111111



**Fig. 6.** Total thermal power generation schedule (6-bus system).

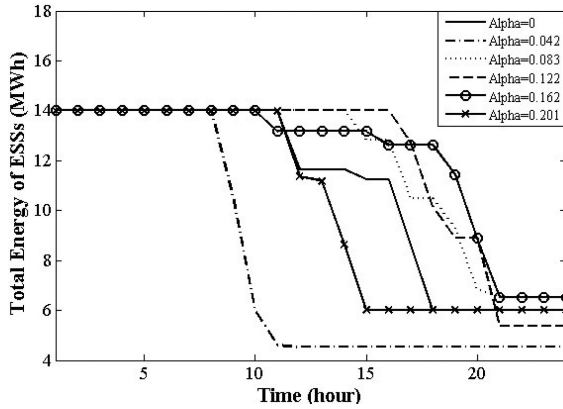


**Fig. 7.** Energy stored in the ESSs (6-bus system).

robustness  $\alpha = 0.201$ . The obtained commitment status of the thermal generating units with their power generation together with the energy stored in ESSs ( $\sigma = 0.3, \alpha = 0.122$ ) are depicted in Table III, and Figs. 6 and 7. As Table III shows, the total number of hours that the thermal units must commit has increased in comparison with the base case in order to satisfy the increased load demand. Accordingly, as shown in Fig. 6, the total power generated by the thermal units increases as the load robustness increases. Note that  $\alpha = 0$  represents the base case without any load uncertainty.

### B. IEEE 24-Bus Test System

This case study is presented using a large-scale system, i.e., updated IEEE Reliability Test System [41], which is the updated

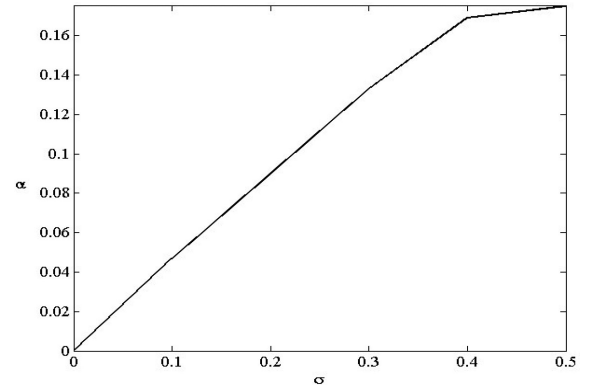


**Fig. 8.** Variations of the load robustness  $\alpha$  versus the cost deviation factor  $\sigma$ , (IEEE 24-bus system).

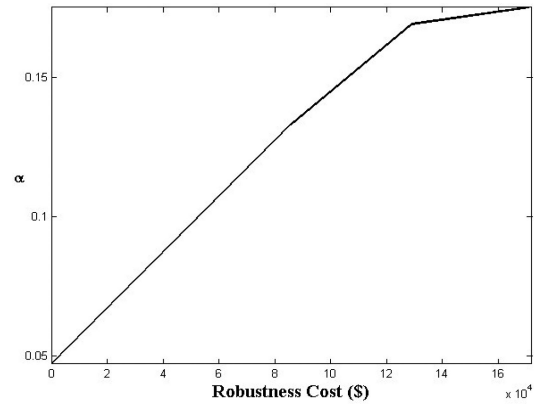


**Fig. 9.** Variation of the load robustness  $\alpha$  versus the robustness cost, (IEEE 24-bus system).

version of the system introduced in [42] to verify the effectiveness of the proposed multiobjective optimization method. In this regard, the generating units of this system are grouped by node and type in order to facilitate the presentation of the results [43]. Hence, the system comprises 17 loads, 12 generating units, and 34 transmission lines.

There are five battery ESSs, which in total account for 10% of the peak load. ESSs are located on buses with the highest local marginal prices (LMPs). In this regard, buses 14, 20, 13, 2, and 1 have the highest LMPs [22]. The capacity of the ESSs is considered as 10% of the peak load demand of the system. In this respect, the base case cost without any uncertainty is \$428 710 for 24 h. Using the IGDT technique for characterizing the load demand uncertainty, Fig. 8 shows the variations of the load robustness for the cost deviation factor. Besides, Fig. 9 indicates the variations of the robustness cost for different values of load robustness. As Fig. 9 shows, the system operator should tolerate higher costs for higher percentages of uncertainty. Fig. 10 depicts the increase in the total thermal power generation with the increase in the load robustness. This means that for further load demand uncertainties, thermal generating units must generate more. Also, Fig. 11 shows the amount of energy stored in ESS units. It is noted that the ESSs units for

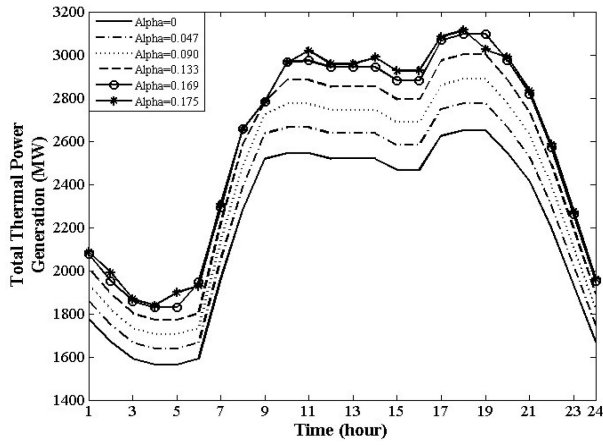


Fig. 10. Total thermal power generation schedule (IEEE 24-bus system).

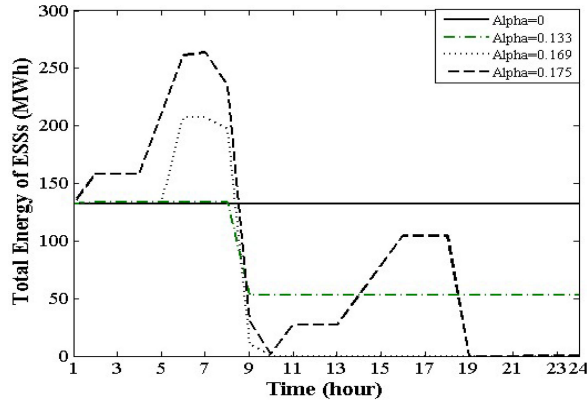


Fig. 11. Energy stored in the ESSs (IEEE 24-bus system).

the base case and cost deviation factors of 10% and 20% remain unused, which is due to the high degradation costs of such units. For higher values of load robustness, the ESSs are supposed to operate in order to contribute to load demand supply.

### C. 118-Bus Test System

In this case, the proposed framework was implemented on a large-scale power system, i.e., a modified IEEE 118-bus test system, which includes 54 thermal units, 186 branches, and 91 load buses. There are five battery ESSs, which in total account for 10% of the peak load. The method used to locate ESSs units is the same as the one used in [22] such that the buses with the highest LMPs are selected for installing ESSs. In this regard, buses 82, 32, 114, 115, and 27 have the highest LMPs. The proposed problem is first solved using a deterministic framework, without any load forecast uncertainty and taking into account the ESS degradation cost. The obtained total operating cost is \$1 366 200. In this case, the ESSs were not scheduled to be used at all, due to their high cost, making their use uneconomical. If the ESS degradation is not considered, the ESSs are scheduled and charged/discharged to support the load demand. Subsequently, the obtained total operating cost is reduced to

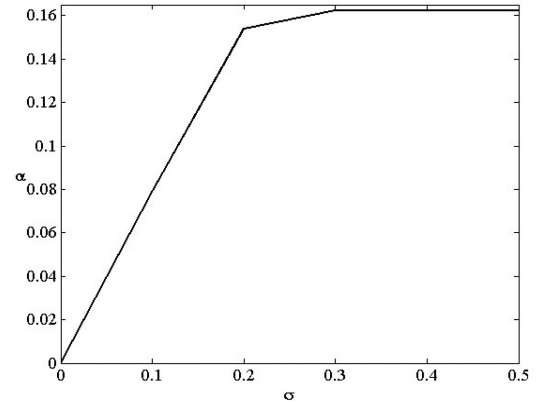


Fig. 12. Variations of the load robustness  $\alpha$  versus the cost deviation factor  $\sigma$ , (IEEE 118-bus system).

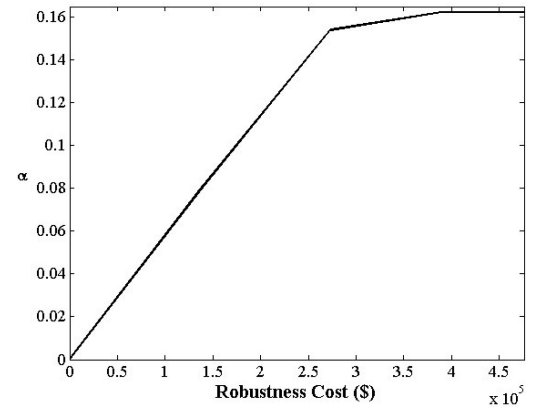


Fig. 13. Variation of the load robustness  $\alpha$  versus the robustness cost, (IEEE 118-bus system).

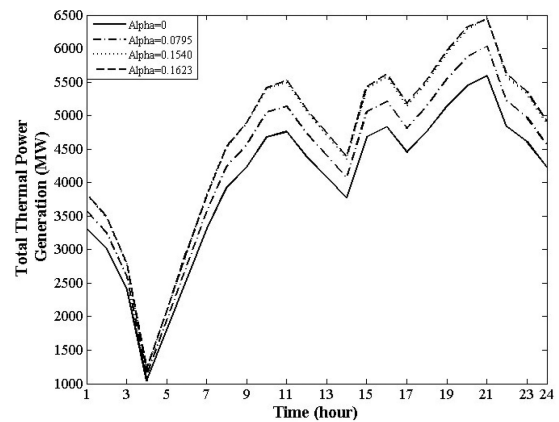


Fig. 14. Total thermal power generation schedule (IEEE 118-bus system).

\$1 358 700. In the case of the load uncertainty, the problem is solved using the proposed IGD technique. Fig. 12 depicts the variation of  $\alpha$  versus  $\sigma$ . As it can be observed from Fig. 12, the load robustness  $\alpha$  increases as the cost deviation factor  $\sigma$  increases up to a point where it saturates. This is due to the fact that in spite of tolerating higher expected costs by the system operator, the technical constraints of the problem do not allow



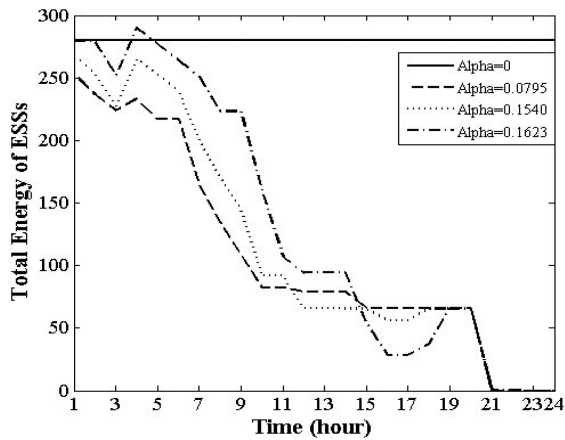


Fig. 15. Energy stored in the ESSs (IEEE 118-bus system).

accommodating higher load demands. Fig. 13 shows the variation of the load robustness  $\alpha$  versus the robustness cost, i.e., the cost that should be tolerated due to the higher deviations of the load demand forecast. The total thermal power generation for different values of load robustness is shown in Fig. 14. Finally, the total energy stored in the ESSs for different values of load robustness is shown in Fig. 15. In the worst case, the ESSs are used to supply the increased load demand.

#### IV. CONCLUSION

This paper investigated the robust day-ahead hourly-based SCUC of generating units in the presence of lithium-ion battery ESSs. The IGDT technique was applied to characterize the load demand uncertainty faced by the system operators. The degradation cost of lithium-ion batteries, as a restricting factor, was calculated and added to the total operating costs. The proposed framework enables the system operator to adjust the degree of conservatism of the operation strategy by changing the value of the cost deviation factor. Advancement of lithium-ion batteries' technology and reduced manufacturing cost will decrease the battery degradation cost, further increasing the attractiveness of utilization of batteries in power systems.

#### REFERENCES

- [1] S. Eckrood and I. Gyuk, "EPRI-DOE handbook of energy storage for transmission & distribution applications," Elect. Power Res. Inst., Inc., Palo Alto, CA, USA, Tech. Rep. EPRI 1001834, pp. 3–35, 2003.
- [2] H. Khorramdel, J. Aghaei, B. Khorramdel, and P. Siano, "Optimal battery sizing in microgrids using probabilistic unit commitment," *IEEE Trans. Ind. Informat.*, vol. 12, no. 2, pp. 834–843, Apr. 2016.
- [3] Y. Zhang, H. H. C. Lu, T. Fernando, F. Yao, and K. Emami, "Cooperative dispatch of BESS and wind power generation considering carbon emission limitation in Australia," *IEEE Trans. Ind. Informat.*, vol. 11, no. 9, pp. 1313–1323, Dec. 2015.
- [4] Q. Zhai, Z. Dong, K. Meng, and J. Ma, "Modelling and analysis of lithium battery operations in spot and frequency regulation service markets in Australia electricity market," *IEEE Trans. Ind. Informat.*, vol. 13, no. 5, pp. 2576–2586, Oct. 2017.
- [5] P. Denholm, E. Ela, B. Kirby, and M. Milligan, "The role of energy storage with renewable electricity generation," Nat. Renewable Energy Lab., Golden, CO, USA, Tech. Rep. NREL/TP-6A2-47187, 2010.
- [6] G. B. Dantzig, "Linear programming under uncertainty," *Manage. Sci.*, vol. 1, pp. 197–206, 1955.
- [7] Y. Ben-Haim, *Info-Gap Decision Theory: Decisions Under Severe Uncertainty*. Orlando, FL, USA: Academic, 2006.
- [8] K. Zare, M. P. Moghaddam, and M. K. Sheikh-El-Eslami, "Risk-based electricity procurement for large consumers," *IEEE Trans. Power Syst.*, vol. 26, no. 4, pp. 1826–1835, Nov. 2011.
- [9] A. Soroudi and M. Ehsan, "IGDT based robust decision making tool for DNOs in load procurement under severe uncertainty," *IEEE Trans. Smart Grid*, vol. 4, no. 2, pp. 886–895, Jun. 2013.
- [10] S. Dehghan, A. Kazemi, and N. Amjady, "Multi-objective robust transmission expansion planning using information-gap decision theory and augmented  $\epsilon$ -constraint method," *IET Gener., Transmiss., Distrib.*, vol. 8, pp. 828–840, 2014.
- [11] M. Kazemi, B. Mohammadi-Ivatloo, and M. Ehsan, "Risk-constrained strategic bidding of GenCos considering demand response," *IEEE Trans. Power Syst.*, vol. 30, no. 1, pp. 376–384, Jan. 2015.
- [12] A. Rabiee, A. Soroudi, and A. Keane, "Information gap decision theory based OPF with HVDC connected wind farms," *IEEE Trans. Power Syst.*, vol. 30, no. 6, pp. 3396–3406, Nov. 2015.
- [13] M. Charwand, A. Ahmadi, A. M. Sharaf, M. Gitzadeh, and A. E. Nezhad, "Robust hydrothermal scheduling under load uncertainty using information gap decision theory," *Int. Trans. Elect. Energy Syst.*, vol. 26, pp. 464–485, 2016.
- [14] K. Chen, W. Wu, B. Zhang, and H. Sun, "Robust restoration decision-making model for distribution networks based on information gap decision theory," *IEEE Trans. Smart Grid*, vol. 6, no. 2, pp. 587–597, Mar. 2015.
- [15] C. Murphy, A. Soroudi, and A. Keane, "Information gap decision theory-based congestion and voltage management in the presence of uncertain wind power," *IEEE Trans. Sustain. Energy*, vol. 7, no. 2, pp. 841–849, Apr. 2016.
- [16] S. Shafiee, H. Zareipour, A. M. Knight, N. Amjady, and B. Mohammadi-Ivatloo, "Risk-constrained bidding and offering strategy for a merchant compressed air energy storage plant," *IEEE Trans. Power Syst.*, vol. 32, no. 2, pp. 946–957, Mar. 2017.
- [17] L. Zhang and Y. Li, "Optimal energy management of wind-battery hybrid power system with two-scale dynamic programming," *IEEE Trans. Sustain. Energy*, vol. 4, no. 3, pp. 765–773, Jul. 2013.
- [18] I. Duggal and B. Venkatesh, "Short-term scheduling of thermal generators and battery storage with depth of discharge-based cost model," *IEEE Trans. Power Syst.*, vol. 30, no. 4, pp. 2110–2118, Jul. 2015.
- [19] A. Gabash and P. Li, "Flexible optimal operation of battery storage systems for energy supply networks," *IEEE Trans. Power Syst.*, vol. 28, no. 3, pp. 2788–2797, Aug. 2013.
- [20] F. Luo, K. Meng, Z. Y. Dong, Y. Zheng, Y. Chen, and K. P. Wong, "Co-ordinated operational planning for wind farm with battery energy storage system," *IEEE Trans. Sustain. Energy*, vol. 6, no. 1, pp. 253–262, Jan. 2015.
- [21] N. Li, C. Uçkun, E. M. Constantinescu, J. R. Birge, K. W. Hedman, and A. Botterud, "Flexible operation of batteries in power system scheduling with renewable energy," *IEEE Trans. Sustain. Energy*, vol. 7, no. 2, pp. 685–696, Apr. 2016.
- [22] M. Parvania, M. Fotuhi-Firuzabad, and M. Shahidehpour, "Comparative hourly scheduling of centralized and distributed storage in day-ahead markets," *IEEE Trans. Sustain. Energy*, vol. 5, no. 3, pp. 729–737, Jul. 2014.
- [23] I. Blanco and J. M. Morales, "An efficient robust solution to the two-stage stochastic unit commitment problem," *IEEE Trans. Power Syst.*, vol. 32, no. 6, pp. 4477–4488, Nov. 2017.
- [24] Y. Zhang, J. Wang, B. Zeng, and Z. Hu, "Chance-constrained two-stage unit commitment under uncertain load and wind power output using bilinear benders decomposition," *IEEE Trans. Power Syst.*, vol. 32, no. 5, pp. 3637–3647, Sep. 2017.
- [25] C. Shao, X. Wang, M. Shahidehpour, X. Wang, and B. Wang, "Security-constrained unit commitment with flexible uncertainty set for variable wind power," *IEEE Trans. Sustain. Energy*, vol. 8, no. 3, pp. 1237–1246, Jul. 2017.
- [26] H. Quan, D. Srinivasan, and A. Khosravi, "Incorporating wind power forecast uncertainties into stochastic unit commitment using neural network-based prediction intervals," *IEEE Trans. Neural Netw. Learn. Syst.*, vol. 26, no. 9, pp. 2123–2135, Sep. 2015.
- [27] Y. Wang, S. Zhao, Z. Zhou, A. Botterud, Y. Xu, and R. Chen, "Risk adjustable day-ahead unit commitment with wind power based on chance constrained goal programming," *IEEE Trans. Sustain. Energy*, vol. 8, no. 2, pp. 530–541, Apr. 2017.
- [28] Á. Lorca and X. A. Sun, "Multistage robust unit commitment with dynamic uncertainty sets and energy storage," *IEEE Trans. Power Syst.*, vol. 32, no. 3, pp. 1678–1688, May 2017.

- [29] J. Aghaei *et al.*, "Optimal robust unit commitment of CHP plants in electricity markets using information gap decision theory," *IEEE Trans. Smart Grid*, vol. 8, no. 5, pp. 2296–2304, Sep. 2017.
- [30] B. Mohammadi-Ivatloo, H. Zareipour, N. Amjadi, and M. Ehsan, "Application of information-gap decision theory to risk-constrained self-scheduling of GenCos," *IEEE Trans. Power Syst.*, vol. 28, no. 2, pp. 1093–1102, May 2013.
- [31] A. Barré, B. Deguilhem, S. Grolleau, M. Gérard, F. Suard, and D. Riu, "A review on lithium-ion battery ageing mechanisms and estimations for automotive applications," *J. Power Sources*, vol. 241, pp. 680–689, Nov. 1, 2013.
- [32] J. Vetter *et al.*, "Ageing mechanisms in lithium-ion batteries," *J. Power Sources*, vol. 147, pp. 269–281, Sep. 9, 2005.
- [33] H. Farzin, M. Fotuhi-Firuzabad, and M. Moeini-Aghaie, "A practical scheme to involve degradation cost of lithium-ion batteries in vehicle-to-grid applications," *IEEE Trans. Sustain. Energy*, vol. 7, no. 4, pp. 1730–1738, Oct. 2016.
- [34] B. Zhou, X. Liu, Y. Cao, C. Li, C. Y. Chung, and K. W. Chan, "Optimal scheduling of virtual power plant with battery degradation cost," *IET Gener., Transmiss., Distrib.*, vol. 10, pp. 712–725, 2016.
- [35] C. Ju, P. Wang, L. Goel, and Y. Xu, "A two-layer energy management system for microgrids with hybrid energy storage considering degradation costs," *IEEE Trans. Smart Grid*, to be published, May 2017.
- [36] C. Zhou, K. Qian, M. Allan, and W. Zhou, "Modeling of the cost of EV battery wear due to V2G application in power systems," *IEEE Trans. Energy Convers.*, vol. 26, no. 4, pp. 1041–1050, Dec. 2011.
- [37] S. B. Peterson, J. Apt, and J. F. Whitacre, "Lithium-ion battery cell degradation resulting from realistic vehicle and vehicle-to-grid utilization," *J. Power Sources*, vol. 195, pp. 2385–2392, Apr. 15, 2010.
- [38] SAFT SA. Intensium Flex, Product Brochure, 2008. [Online]. Available: <http://www.saftbatteries.com/battery-search/intensium%C2%AE-flex>. Accessed on: Jan. 31, 2014.
- [39] Z. Yuan and C. Mo-Yuen, "Microgrid cooperative distributed energy scheduling (CoDES) considering battery degradation cost," in *Proc. IEEE 25th Int. Symp. Ind. Electron.*, 2016, pp. 720–725.
- [40] "Case studies: Battery storage," 2015. [Online]. Available: [www.IRENA.org](http://www.IRENA.org)
- [41] C. Ordoudis, P. Pinson, J. M. Morales, and M. Zugno, "An updated version of the IEEE RTS 24-bus system for electricity market and power system operation studies," Tech. Univ. of Denmark, Lyngby, Denmark, Tech. Rep., 2016.
- [42] C. Grigg *et al.*, "The IEEE reliability test system-1996. A report prepared by the reliability test system task force of the application of probability methods subcommittee," *IEEE Trans. Power Syst.*, vol. 14, no. 3, pp. 1010–1020, Aug. 1999.
- [43] J. M. Morales, A. J. Conejo, K. Liu, and J. Zhong, "Pricing electricity in pools with wind producers," *IEEE Trans. Power Syst.*, vol. 27, no. 3, pp. 1366–1376, Aug. 2012.

Authors' photographs and biographies not available at the time of publication.